Dynamic and structural studies on 1,2,3-trichloropropane in the solid phase

1991 J. Phys.: Condens. Matter 3 2287

(http://iopscience.iop.org/0953-8984/3/14/008)

J. Phys.: Condens. Matter 3 (1991) 2287–2298. Printed in the UK

Dynamic and structural studies on 1,2,3-trichloropropane in the solid phase

Mariano J Zuriaga†, Gustavo A Monti‡ and Carlos A Martín†
Facultad de Matematica, Astronomia y Fisica, Universidad Nacional de Cordoba, Laprida 854, 5000-Cordoba, Argentina

Received 9 November 1990

Abstract. ^{35}Cl nuclear quadrupole resonance (NQR) frequencies ν_Q and spin–lattice relaxation times T_1 were measured between 100 and 250 K in 1,2,3-trichloropropane ($CH_2ClCHClCH_2Cl$). Three narrow lines were detected in the stable solid phase, indicating that only one of the six possible conformers is present. Also, the three lines were assigned to the three chlorine atoms in the molecule from their distinct temperature behaviours. The dominant mechanism responsible for the relaxation above 200 K is proposed to be the reorientational motion of the CH_2Cl end groups, and activation energies of 32.5 and 49.0 kJ mol^{-1} are determined for the two end groups. The ^1H nuclear magnetic resonance lineshape $f(H)$ shows a structure due to the dipolar interaction between the protons of the CH_2Cl groups. From the analysis of $f(H)$ a distance $d_{HH} = 1.68$ Å is obtained, which turns out to be quite close to that already determined in solid dichloroethane. Fast cooling of the sample from the liquid state produces very broad NQR signals. The results of differential thermal analysis seem to indicate the existence of a glassy state with a characteristic $T_g = 144$ K.

1. Introduction

1,2,3-trichloropropane (TCP) belongs to the family of halogenated propanes, and has previously been investigated by means of vibrational spectroscopy (Thorbjørnsrud *et al* 1973, Gustavsen *et al* 1978) and gaseous electron diffraction (Farup and Stølevik 1974). The 1,2,3-trihalopropanes with identical halogens have six possible staggered conformations. They are named A (*anti*) and G (*gauche*) according to the position of the vicinal halogens (Thorbjørnsrud *et al* 1973). Of these theoretical conformers, three have been detected in TCP in the vapour phase (Farup and Stølevik 1974) with relative concentrations of 68%, 28% and 4% for AG_-, AG_+ and G_+G_-, respectively, and they are shown in figure 1. Spectroscopic studies (Thorbjørnsrud *et al* 1973) verified the existence of these conformers in the liquid at room temperature, but only one was present in the low-temperature and high-pressure crystals. Though the abundant conformers of TCP could not be identified by vibrational spectroscopy, it was concluded that the most abundant conformer of the vapour also dominates in the liquid, and that it is the only one that remains in the crystal.

Since nuclear quadrupole resonance (NQR) is a very useful technique for studying static and dynamic properties of solids, we have measured $\nu_Q(T)$ and $T_1(T)$ to examine

† Fellow of CONICET.
‡ Holder of a fellowship of CONICET.

0953-8984/91/142287 + 12 $03.50

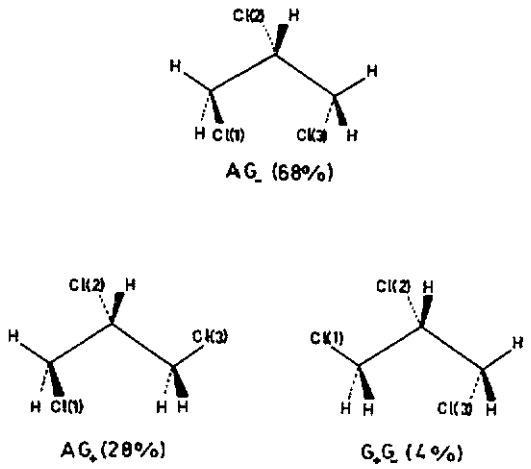

Figure 1. The TCP conformers present in the liquid state. The numbers in parentheses, which indicate the relative abundances at 330 K, and the notation are taken from Farup and Stølevik (1974).

the possibility of the existence of more than one conformer, and as well as to study the motion of the CH_2Cl end groups. The ^1H nuclear magnetic resonance (NMR) lineshape was analysed to obtain information about the CH_2Cl structure and to compare it with data obtained by other techniques.

Furthermore, it is known that many straight-chain organic compounds are capable of existing in more than one form in the solid state, depending not only upon the compound itself but also upon its previous thermal history, as has been observed in some n-alkyl bromides (Kushner *et al* 1950, Crowe and Smyth 1950). Differential thermal analysis (DTA) traces were recorded and, depending upon the thermal history, glass-like transitions are detected.

2. Experimental details

A TCP liquid sample, provided by Fluka (catalogue number 91380), was used as received. High-resolution NMR spectra show that impurities of CH_2 and CH_3 were less than 1%. The sample was sealed into a glass bottle under vacuum.

The ^{35}Cl NQR frequencies were measured by means of a super-regenerative type spectrometer with an uncertainty of about 500 Hz. The spin–lattice relaxation times were measured by means of a fast Fourier transform (FFT) pulsed spectrometer with an overall error of 5% using the $\pi/2$–τ–$\pi/2$ pulse sequence. Copper–constantan thermocouples were used for the control and measurements of temperature, and the latter was determined with an accuracy of 0.25 K. NMR lineshapes were measured with a continuous-wave Robinson-type spectrometer. The DTA traces were determined with a home-made apparatus (Martín 1982).

3. Differential thermal analysis

3.1. Results

At this point we describe the DTA results prior to more detailed investigations. DTA experiments were carried out on a specimen that was cooled down to about liquid-nitrogen temperature in two different ways: (i) slow cooling at a rate of 0.25 K min^{-1},

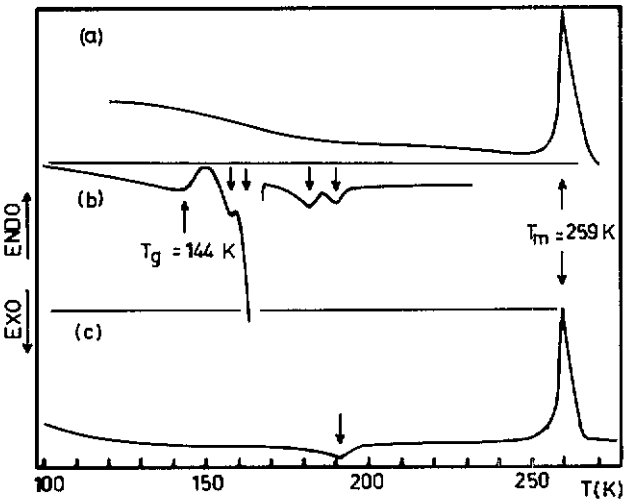

Figure 2. The DTA traces for TCP: (*a*), (*b*) and (*c*) correspond to different thermal histories, as explained in the text.

and (ii) rapid cooling from the liquid state at room temperature down to 77 K by plunging the specimen into liquid nitrogen.

The DTA traces, on heating, are shown in figure 2. It is found that no solid–solid phase transitions occur in the slowly cooled sample; only an endothermic peak due to melting appears at T_m = 259 K (figure 2(*a*)). In the rapidly cooled specimen several anomalies appear in the range from 140 to 195 K (figure 2(*b*)).

It should be noted that these anomalies only appear when the sample is quenched down to liquid-nitrogen temperature. If the fast-cooled sample is heated to 190 K and then cooled down again, it is seen that only the anomalies near 190 K remain (figure 2(*c*)).

3.2. Discussion

At about 140 K, in the fast-cooled specimen, a change in ΔT appears, as if some type of transition is beginning to take place. About 155 K the specimen undergoes a spontaneous change with evolution of heat. It is evident that by rapid cooling an unstable form may be frozen-in; and not until the temperature rises does this form change over to the more stable one.

These phenomena may be compared with that which occurs in some glasses. Supercooled liquids, at low enough temperatures, almost invariably exhibit a pseudo-second-order thermodynamic transition, which is commonly known as the 'glass transition'. We may then say that TCP is a glass-forming liquid, like other common organic liquids (Adam and Gibbs 1965, Angell *et al* 1978).

On fast cooling, TCP forms a glass at low temperatures. On warming, the usual glass transformation begins to take place, but a temperature is soon reached where the crystallization is spontaneous. This behaviour is quite similar to that occurring in i-butyl bromide (Baker and Smith 1939), n-amyl bromide (Kushner *et al* 1950) and some polymers (Cheng and Wunderlich 1988). A glass temperature T_g = 144 K was determined from the DTA traces by the usual methods (Pope and Judd 1980).

The analysis of the DTA traces for the fast-cooled specimen (figure 2(*b*)) reveals the existence of two double-peaked exothermic processes, as well as an endothermic one.

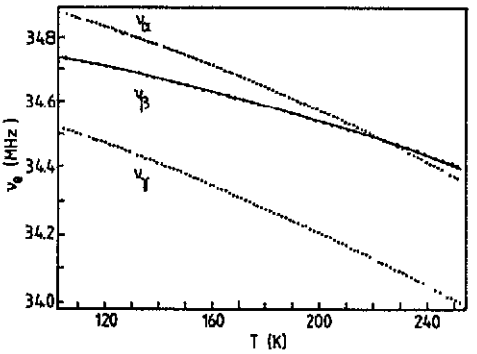

Figure 3. Temperature dependence of the three ^{35}Cl NQR frequencies detected in TCP in the slowly cooled sample. The full curve corresponds to the values produced with equation (1*a*) with the parameters shown in table 1. The difference between the fit and the data values is smaller than 700 Hz.

The endotherm step at 144 K corresponds to the glass transition. The first sharp exothermic peak at 160 K corresponds to the spontaneous crystallization. This exotherm shows a double-peaked structure, which is probably due to the presence of impurities in the sample (Cervinka and Hruky 1982). The second double exothermic peak could be associated with the passage from the relative abundance of the conformers in the liquid state to that in the solid stable phase. However, this double peak is not well understood, because its position is quite sensitive to the heating and cooling rates. We have obtained three sets of values for their temperatures: 185–192 and 182–190 K in two runs (figure 2(*b*) is one of them) and a broad peak at 191 K with a shoulder at 185 K in the case in figure 2(*c*). This is not the case for the other transition temperatures.

4. Nuclear quadrupole resonance frequency

4.1. Results

The NQR spectrum exhibits three lines, of the same intensity, whose temperature dependences (ν_Q versus T) were measured in the range 100–250 K; the data are depicted in figure 3. These lines are referred to as $\nu_\alpha > \nu_\beta > \nu_\gamma$, on the low-temperature side. Although the melting point is 259 K, they broadened beyond detection above 250 K. These three lines were only detected in the slowly cooled sample. In the rapidly cooled sample, no signals were detected below 160 K, therefore indicating that the sample is not in a crystalline form (glassy state). Above the first exothermic peak, broad NQR signals ($\delta\nu > 20$ kHz) were observed at roughly the same frequencies as those in the slowly cooled sample.

For all the possible conformers (figure 1) the three chlorine atoms are chemically inequivalent, leading to three different NQR frequencies, as is observed. The existence of only three equally intense lines of width $\delta\nu \simeq 2.5$ kHz confirms the conclusion, based on far-infrared and Raman spectroscopy, that only one conformer is present in the crystalline stable form (AG_-) (Thorbjørnsrud *et al* 1973), since it is well known that orientational type of disorder produces broad NQR signals in crystalline samples (Rubinstein and Taylor 1974).

It may be seen in figure 4 that ν_α versus T and ν_γ versus T are essentially parallel, i.e. their temperature derivatives are almost equal ($\simeq -2.9$ kHz K^{-1}) for all of the

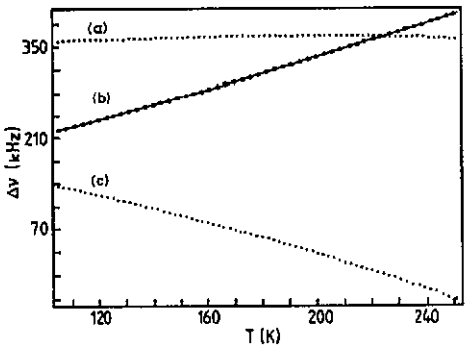

Figure 4. Temperature dependences of the differences among the three NQR frequencies depicted in figure 3: (*a*) $\Delta\nu = \nu_\alpha - \nu_\gamma$, (*b*) $\Delta\nu = \nu_\beta - \nu_\gamma$, (*c*) $\Delta\nu = \nu_\alpha - \nu_\beta$. The full curve corresponds to the values produced by equation (3) with the parameters shown in table 2. The difference between the fit and the data values is smaller than 1 kHz.

temperature range; and that the derivative for ν_β is smaller ($\simeq -2.0$ kHz K^{-1}) than those for ν_α and ν_γ. The ν_α and ν_β lines cross each other around 224.5 K.

4.2. Discussion

The temperature dependences of the resonance frquencies may be accounted for by the Bayer–Kushida theory (Kushida *et al* 1956). The temperature dependence of $\nu_Q(T)$ is primarily due to the librational motions of the molecule as a rigid body. The intramolecular vibrations are not so effective in averaging the electric field gradient (EFG), but in this case some additional vibrational modes involving the CH_2Cl groups must be taken into consideration to explain why the temperature coefficients in ν_α and ν_β are larger than that in ν_γ. Among such additional modes the most dominant contribution comes from the internal out-of-plane torsional mode of the CH_2Cl groups about the C–C axes. The frequencies of the torsional modes are lower than those associated with the other internal modes (Thorbjørnsrud *et al* 1973); therefore these modes will be more effective in averaging the EFG.

As mentioned above, the conformation adopted by the molecules in the stable solid state is denoted by AG_- and shown in figure 1. From the ν_Q versus T behaviour it is clear that ν_β corresponds to Cl(2), the one attached to the central C(2) as shown in figure 1; also, ν_α and ν_γ are associated with either Cl(1) or Cl(3).

The behaviour of $\nu_Q(T)$ may be described to a good approximation by the following expressions:

$$\nu_\beta = \nu_{\beta 0}\left\{1 - \frac{3\hbar}{8\pi c}\frac{A_e}{\omega_e}\coth\left(\frac{hc\omega_e}{2k_BT}\right)\right\} \tag{1a}$$

$$\nu_\alpha = \nu_{\alpha 0}\left\{1 - \frac{3\hbar}{8\pi c}\left[\frac{A_e}{\omega_e}\coth\left(\frac{hc\omega_e}{2k_BT}\right) + \frac{A_t}{\omega_t}\coth\left(\frac{hc\omega_t}{2k_BT}\right)\right]\right\} \tag{1b}$$

$$\nu_\gamma = \nu_{\gamma 0}\left\{1 - \frac{3\hbar}{8\pi c}\left[\frac{A_e}{\omega_e}\coth\left(\frac{hc\omega_e}{2k_BT}\right) + \frac{A_t}{\omega_t}\coth\left(\frac{hc\omega_t}{2k_BT}\right)\right]\right\}. \tag{1c}$$

Here the ν_{i0} are the rigid lattice NQR frequencies, ω_e and ω_t are the effective librational and torsional frequencies (Kushida *et al* 1956) (in cm^{-1}) respectively, and A_e and A_t are

Table 1. Values obtained for the parameters by fitting equation (1*a*) to the frequency data.

ω_{e0} (cm^{-1})	76.9
g_e (K^{-1})	7.44×10^{-4}
$\nu_{\beta 0}$ (kHz)	34913.0
I_{eff}^{-1} (amu Å^2)$^{-1}$	6.37×10^{-3}

Table 2. Values obtained for the parameters by fitting equation (3) to the frequency difference data.

ω_{t0} (cm^{-1})	101.7
$\Delta\nu_0$ (kHz)	72.7
I_{tors} (amu Å^2)	86.4

the inverse of the effective moments of inertia for the corresponding normal modes defined as

$$A_e = \frac{1}{I_{eff}} \sum_{i=1}^{3} \frac{\sin^2 \alpha_i}{I_i} \qquad \text{and} \qquad A_t = \frac{\sin^2 \alpha}{I_{tors}} \tag{2}$$

where I_i is the ith principal moment of inertia of the molecule, α_i is the angle between the ith principal axis of inertia and the C–Cl bonds (Hasting and Oja 1972) and I_{tors} is the reduced moment of inertia of the CH_2Cl group; c is the speed of light (in cm s^{-1}) while h, $\hbar$ and k_B have their standard meanings.

Following Brown's suggestion (Brown 1960) we assumed that in the quasi-harmonic approximation $\omega_e = \omega_{e0}(1 - g_e T)$. Fitting equation (1*a*) to the ν_β data, the values for the parameters ω_{e0}, g_e, $\nu_{\beta 0}$ and A_e are deduced, and these are shown in table 1.

Assuming that the contributions of the librations are equal for ν_α, ν_β and ν_γ, we can deduce the excess temperature coefficient of ν_α and ν_γ lines, which may be interpreted as arising from the internal out-of-plane torsional mode. Then from equations (1*a*) and (1*c*)

$$\nu_\gamma - \nu_\beta = \Delta\nu_0 - \nu_{0\gamma} \frac{3\hbar}{8\pi c} \frac{A_t}{\omega_t} \coth\left(\frac{hc\omega_t}{2k_B T}\right). \tag{3}$$

A similar expression holds for the difference between ν_α and ν_β. A temperature-dependent term on the right-hand side of equation (3) has been neglected because it is $\Delta\nu_0/\nu_{0\gamma}$ times smaller than the second term on the right-hand side of equation (3).

Fitting the data by means of equation (3), the parameters shown in table 2 are obtained. Making the same fit with the $\nu_\alpha - \nu_\beta$ difference, unreliable values for the parameters are obtained. A possible explanation of this fact is given below.

The values shown in tables 1 and 2 provide an excellent description of the ν_Q versus T data, as may be seen in figures 2 and 3. The two CH_2Cl torsional frequencies (Gustavsen *et al* 1978) in the AG_- conformer are 80 and 152 cm^{-1}, yielding an average value (defined by Zuriaga and Martín (1986) as $\bar{\omega}_t^{-2} = N^{-1}\Sigma_i\, \omega_{ti}^{-2}$) of $\omega_t = 100$ cm^{-1}, a value very close to that determined from these analyses, as shown in table 2. Infrared and Raman spectra show four low-frequency bands in solid TCP (Thorbjørnsrud *et al* 1973) at 156, 135, 93 and 75 cm^{-1}, which are tentatively attributed to torsional modes, noting that some of them could be connected with external modes. As the lowest frequency detected is

75 cm^{-1} and the effective librational frequency determined by equation (1) is 77 cm^{-1}, some librations must lie below 70 cm^{-1}. The temperature coefficient g_e has a typical value for molecular crystals.

The torsional moment of inertia determined by means of equation (3) is quite similar to the geometrical value $I_{tors} = 80.9$ amu Å^2; however, the value determined for A_e turns out to be ≈40% larger than that calculated for Cl(2) by using the structural data (Farup and Stølevik 1974); this is due to the fact that not all C–Cl bending modes are accounted for in equation (1*a*).

The A_e values calculated from equation (2) using the structural data are 4.78×10^{-3}, 4.70×10^{-3} and 6.03×10^{-3} amu^{-1} Å^{-2} for the chlorines situated at positions 1, 2 and 3, respectively. Equations (1) and (3) and the similar one for $\nu_\alpha - \nu_\beta$ are based on the hypothesis that the average contribution of all the librational modes is the same for the three ν_Q, i.e. there is only one value for A_e. However, on the basis of the above calculated values for A_e it turns out that only $\nu_\alpha - \nu_\beta$ versus T or $\nu_\gamma - \nu_\beta$ versus T will be adequately described by an equation similar to equation (3). In fact, as was mentioned above, a set of meaningful parameters is determined when fitting $\nu_\gamma - \nu_\beta$ versus T with equation (3), while that is not the case when one attempts to fit $\nu_\alpha - \nu_\beta$ versus T with an equation similar to equation (3). These analyses allow us to produce an assignment as to what Cl atoms are associated with the three lines of the NQR spectrum, namely Cl(1) to ν_γ, Cl(2) to ν_β and Cl(3) to ν_α. Additionally, these analyses provide further support for the approximations leading to equations (1) and (3).

5. Spin–lattice relaxation time

5.1. Results

The spin–lattice relaxation time T_1 was measured from 85 to 250 K for all three resonance lines, and the results are shown in figure 5. Two well defined temperature regions may be distinguished, for all three lines. Below 200 K, T_1 behaves normally, indicating that the dominant relaxation mechanism is that due to the anharmonicities of the lattice normal modes of vibration, mainly those of the librational modes. Above that temperature, a dramatic shortening of T_1 occurs, indicating the onset of a very efficient thermally activated process.

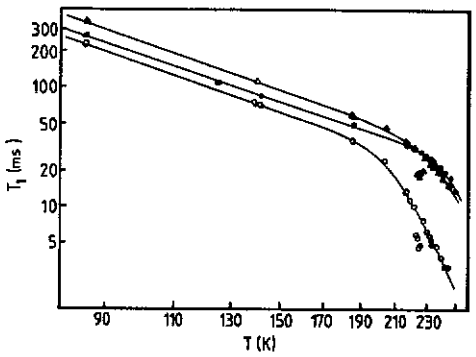

Figure 5. Temperature dependences of the spin–lattice relaxation times for the three ^{35}Cl NQR lines detected in TCP (○, △ and ● correspond to ν_α, ν_β and ν_γ respectively). The full curves indicate the values generated by using equation (4) with the values given in table 3.

Table 3. Values obtained for the parameters by fitting equation (4) to the T_1 versus T data. The assignation made is also indicated.

Line	Assignment	a (10^{-4} s^{-1})	λ	E_a (kJ mol^{-1})
ν_α	Cl(3)	2.04	2.25	32.5
ν_β	Cl(2)	1.43	2.24	32.5
ν_γ	Cl(1)	2.35	2.18	49.0

It must be pointed out that ν_α and ν_β lines began to overlap with each other about 5 K below their crossing temperature (224.5 K). Therefore, in this temperature range, the cross-relaxation process between these lines works so as to shorten their relaxation time (Abragam 1970, p 154, Bloembergen *et al* 1959), as may be observed in figure 5.

5.2. Discussion

The relaxation time for all three lines may be described, except in the neighbourhood of the ν_α and ν_β crossing temperature, as

$$T_1^{-1} = aT^\lambda + b\exp(E_a/RT). \tag{4}$$

The first term on the right-hand side of equation (4) represents the contribution from lattice vibrations (Chihara and Nakamura 1981) and the second term corresponds to a molecular reorientational process (Alexander and Tzalmona 1965) having activation energy E_a. The best-fit parameters λ and E_a were determined by using non-linear least-squares methods and are shown in table 3. The λ values are very similar for the three lines, as expected from the relaxation mechanism driven by lattice vibrations (Chihara and Nakamura 1981).

Since the activation energies E_a are so different, the thermally activated process must be associated with the stochastic reorientations of the CH_2Cl end groups rather than those of the molecule as a whole. Reorientations of the CH_2Cl groups between asymmetric double-minimum potential wells separated from each other by 120° are possible, giving rise to the conformers AG_+ and G_+G_- shown in figure 1.

According to the strong collision theory (Alexander and Tzalmona 1965) the time evolution of the nuclear polarization P^i ($i = 1, 2$) at site i of the double-minimum potential is given by

$$P^i - \langle P^i\rangle = c_{i\mathrm{I}}\exp(-t/T_1^{\mathrm{I}}) + c_{i\mathrm{II}}\exp(-t/T_1^{\mathrm{II}}) \tag{5}$$

where $\langle P^i\rangle$ is the equilibrium polarization, and $c_{i\mathrm{I}}$, $c_{i\mathrm{II}}$, T_1^{I} and T_1^{II} are functions of the jump angle and the transition probabilities from the equilibrium site to the metastable site ($w_{i'i}$) and the opposite one ($w_{ii'}$). The following relations

$$w_{ii'} = w_{i'i}\exp(\Delta E/RT) \qquad \text{and} \qquad \tau_c^{-1} = w_{i'i} = \tau_0^{-1}\exp(-E/RT)$$

hold, with ΔE the energy difference between the two minima and E being the barrier height. In the case that $w_{ii'} \gg w_{i'i}$ then only the first term on the right-hand side of equation (5) remains and $1/T_1^{\mathrm{I}} = \frac{8}{3}\tau_c^{-1} + \mathrm{O}(w_{i'i}^2/w_{ii'})$, corresponding to the second term on the right side of equation (4). In this case only the height of the barrier E, and not the potential difference between the two minima, may be determined.

As we can see in figure 1, a 120° rotation of the $CH_2Cl(3)$ group in the AG_- conformer about the axis C(2)–C(3) leads to the AG_+ conformer, and a similar rotation of the

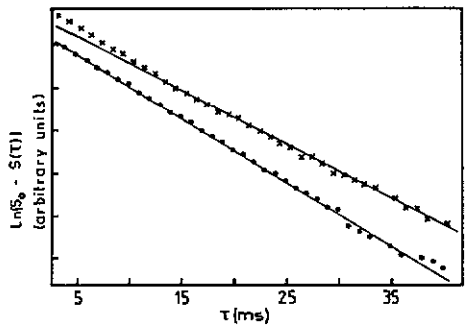

Figure 6. Time behaviour of the magnetization after a $\pi/2$–τ–$\pi/2$ pulse sequence. The full circles correspond to the ν_α line at 216.5 K, and the crosses correspond to the ν_α and ν_β lines at 225.4 K.

$CH_2Cl(1)$ to the G_+G_- one. Since G_+G_- is energetically less favourable than the AG_+ configuration, it is reasonable to expect that the activation energy for the reorientation of the $CH_2Cl(3)$ group will turn out to be smaller than that for the $CH_2Cl(1)$ group. These analyses are in excellent agreement with the results shown in table 3, also bringing additional support to the assignment based upon the analysis of ν_Q versus T.

The Cl(2) nucleus experiences EFG fluctuations resulting from the reorientations of the two nearby CH_2Cl groups, therefore providing an additional relaxation mechanism ($T_{1\mathrm{mod}}$). The expression for $T_{1\mathrm{mod}}$ may be obtained from Woessner and Wutowsky (1963). The evaluation of the correlation functions of the components of the EFG tensor, V_μ ($-2 \leqslant \mu \leqslant 2$), must be done bearing in mind that the EFG fluctuations are due to the reorientations of the two nearby CH_2Cl groups between the asymmetric double-minimum potential wells. Thus,

$$T_{1\mathrm{mod}}^{-1} = \frac{e^2Q^2}{6\hbar^2}(4|\Delta V_{\pm1}|^2 + |\Delta V_{\pm2}|^2)\frac{w_{i'i}w_{ii'}}{(w_{i'i} + w_{ii'})}[(w_{i'i} + w_{ii'})^2 + \omega_Q^2]^{-1}$$

where Q is the scalar quadrupole moment of the Cl nucleus, e is the proton charge, ω_Q is the NQR resonance frequency of the Cl(2) nucleus and ΔV_μ indicates the difference in the components of the EFG (V_μ) at the Cl(2) site due to the reorientations of the CH_2Cl groups between the two minima. In the slow-motion limit the above equation becomes

$$T_{1\mathrm{mod}}^{-1} = \frac{e^2Q^2}{6\hbar^2\omega_Q^2}(4|\Delta V_{\pm1}|^2 + |\Delta V_{\pm2}|^2)w_{i'i}. \tag{6}$$

This equation leads to the exponential behaviour shown in equation (3). Actually, $T_{1\mathrm{mod}}$ includes two terms like equation (6), owing to the fact that the modulations of the EFG are produced by the reorientation of both CH_2Cl groups, each of them with different E_a. The E_a obtained for Cl(2) is equal to that corresponding to Cl(3), therefore indicating that the EFG at the Cl(2) site is more heavily affected by the reorientations of the CH_2Cl group at the *gauche* (G) position than by that at the *anti* (A) position.

It is observed from figure 5 that near 225 K the spin–lattice relaxation times for ν_α and ν_β look smaller than those that should correspond to this temperature. Since the crossing of ν_α and ν_β lines occurs at 224.5 K, this decreasing of the spin–lattice relaxation times must be associated with a cross-relaxation mechanism between the two spin systems. When the cross-relaxation is present, the time evolution of the nuclear polarization is described by a more complex functional form than that of a single exponential, as may be seen in figure 6. As a matter of fact, the evolution of the nuclear polarization

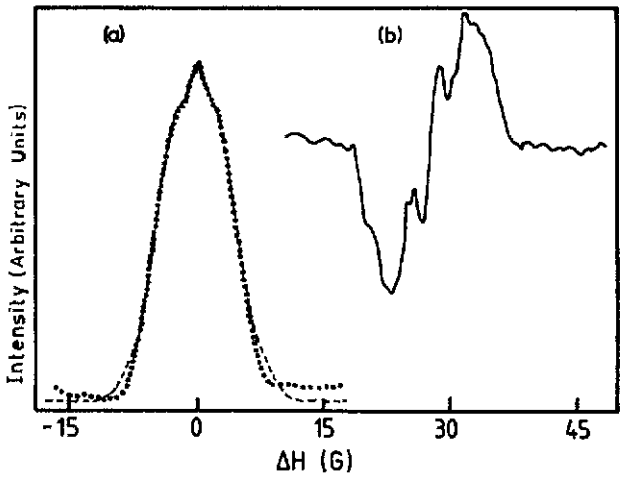

Figure 7. Proton absorption lineshape (*a*) and its first derivative (*b*) at 147 K in TCP. The broken curve corresponds to the values determined using equation (9) with the values for the parameters given in the text.

is described by a double exponential similar to that given by equation (5), and the measured relaxation times ($1/T_1$) do not correspond to the spin–lattice relaxation times. The relationship among the various quantities involved is given by the following expression (Bloembergen *et al* 1959)

$$[(T_1^{\alpha})^{-1} + T_c^{-1} - T_1^{-1}][(T_1^{\beta}) + T_c^{-1} - T_1^{-1}] - T_c^{-2} = 0 \tag{7}$$

where T_1^{α} and T_1^{β} are the spin–lattice relaxation times of each spin system (Cl(2) and Cl(3)), and T_c is the cross-relaxation time for both spin systems. The measured relaxation times turn out to be smaller than the respective spin–lattice relaxation times.

When $\nu_{\alpha} = \nu_{\beta}$ the cross-relaxation time takes its smaller value (Bloembergen *et al* 1959), and in this case it is possible to find a rough value for T_c by interpolating values of T_1^{α} and T_1^{β} at the crossing temperature. In this form the value of $\simeq$55 ms is deduced for T_c.

The NQR lineshapes are generally well described by Lorentzian functional forms and this is assumed to be the case for the ν_{α} and ν_{β} lines. The expression for T_c at the crossing temperature is (Bloembergen *et al* 1959)

$$T_c^{-1} = \frac{9\gamma^4\hbar^2}{16(\Delta\nu_{\alpha} + \Delta\nu_{\beta})} \sum_j (1 - 3\cos^2\theta_{ij})^2 r_{ij}^{-6} \tag{8}$$

where γ is the gyromagnetic ratio of the Cl nucleus, $\Delta\nu_{\alpha}$ and $\Delta\nu_{\beta}$ are the linewidths, and θ_{ij} and r_{ij} are the angle with respect to the z axis and the modulus of the vector connecting Cl(2) and Cl(3), respectively. Since the crystalline structure is not available, only an upper limit for T_c may be obtained by using equation (8) with $r_{ij} =$ 3.39 Å, i.e. the intramolecular Cl(2)–Cl(3) distance. Therefore a value of $\simeq$200 ms is deduced for T_c, which by consideration of the various approximations involved may be taken as a reasonable upper limit for the value of 55 ms deduced from the experimental data, indicating the correctness of the proposed mechanism for T_c.

6. ^{1}H nuclear magnetic resonance lineshape

In figure 7 are shown the measured proton absorption lineshape, $f(H)$, and its derivative, $\partial f(H)/\partial H$, at 147 K. The derivative $\partial f/\partial H$ exhibits two pairs of peaks, while for a simple absorption line the derivative has only one pair of peaks. This situation arises when the nuclear spins in solids form small groups within which the spin separations are distinctly smaller than those between neighbouring groups. Since the dipole–dipole interaction decreases rapidly with distance, to a first approximation one may consider such a group as an isolated system (Abragam 1970 p 221). The resonance line of such a system exhibits a fine structure broadened by the influence of the spins belonging to neighbouring groups. In a TCP molecule two such groups may clearly be distinguished: the central group CHCl(2), and the two end groups $CH_2Cl(1)$ and $CH_2Cl(3)$. In these last groups the shortest H–H distance is (Farup and Stølevik 1974) 1.84 Å (i.e. the H–H intra-group distance), while the distance from the H in the central CHCl(2) group to the nearest H in the end groups is larger than 2.5 Å. Therefore, the absorption line could be described as the superposition of two Pake doublets (those due to $CH_2Cl(1)$ and $CH_2Cl(3)$) and a single line (due to CHCl(2)), i.e.

$$f(\Delta H) = 2\int_{-\infty}^{\infty} F(H_0)S(\Delta H - H_0)\,\mathrm{d}H_0 + (2\pi\beta_1^2)^{-1/2}\exp(-\Delta H^2/2\beta_1^2). \tag{9}$$

Here $F(H_0)$ is the theoretical lineshape of the doublet in a polycrystalline sample, and $S(H)$ represents the dipolar broadening produced by the rest of the lattice and is describable by a Gaussian of width β. The second term on the right-hand side of equation (9) represents the contribution of the H(2) protons.

By fitting the experimental lineshape with equation (9) three parameters were obtained: $\beta = 1.60$ G, $\beta_1 = 1.97$ G and $d_{HH} = 1.68$ Å. The value of d_{HH} is rather smaller than that determined from electron diffraction in gaseous TCP ($d = 1.84$ Å), but is quite close to the value 1.70 Å determined for the protons of the CH_2Cl group in solid dichloroethane (Abragam 1970 p 221). This means that the H–H distances determined in Angell and Rao (1972) are not correct or that in the solid phase the angle HCH is reduced from 108.2° to 95.5° owing to interactions between CH_2Cl groups and the neighbouring molecules.

7. Concluding remarks

By means of the analyses of the NQR parameters we have confirmed that only one conformer of TCP is present in the solid, when this is obtained by slow cooling from the liquid, and that stochastic reorientations of the end groups begin to take place when the temperature rises. These reorientations are proposed to occur about the C(2)–C(3) and C(1)–C(3) axes, therefore producing transitions from the more stable conformer AG_- to the less stable ones AG_+ and G_+G_-, respectively. The assignment of the NQR lines to the three Cl atoms was made, and the temperature dependence of ν_Q well explained by the Bayer model. The DTA and NQR results seem to indicate that TCP is a glass-forming liquid. Further DTA and NQR studies will allow a better understanding of this glassy state.

Acknowledgments

Partial financial support provided by CONICET (Consejo Nacional de Investigaciones Científicas y Técnicas) and CONICOR (Consejo de Investigaciones Científicas y Tecnológicas de la Provincia de Córdoba) is gratefully acknowledged.

References

Abragam A 1970 *The Principles of Nuclear Magnetism* (London: Oxford University Press) pp 154, 221
Adam G and Gibbs J H 1965 *J. Chem. Phys.* **43** 139
Alexander S and Tzalmona A 1965 *Phys. Rev.* A **138** 845
Angell C A and Rao K J 1972 *J. Chem. Phys.* **57** 470
Angell C A, Sare J M and Sare E J 1978 *J. Phys. Chem.* **82** 2622
Baker J and Smith C P 1939 *J. Chem. Phys.* **61** 2063
Bloembergen N, Shapiro S, Pershan P S and Artman J O 1959 *Phys. Rev.* **114** 445
Brown R J C 1960 *J. Chem. Phys.* **32** 116
Cervinka Z and Hruky A 1982 *J. Non Cryst. Solids* **48** 231
Cheng S Z D and Wunderlich B 1988 *Thermochim. Acta* **134** 161
Chihara H and Nakamura N 1981 *Advances in Nuclear Quadrupole Resonance* vol IV (London: Heyden) p 1
Crowe R W and Smyth C P 1950 *J. Chem. Phys.* **72** 1098
Farup P E and Stølevik R 1974 *Acta Chem. Scand.* A **28** 871
Gustavsen J E, Klæboe P and Stølevik R 1978 *J. Mol. Struct.* **50** 285
Hasting R N and Oja T 1972 *Chem. Phys.* **57** 2139
Kushida T, Benedek G B and Bloembergen N 1956 *Phys. Rev.* **104** 1365
Kushner L M, Crowe R W and Smyth C P 1950 *J. Chem. Phys.* **72** 1091
Martín C A 1982 *Proc. Seventh Int. Conf. on Thermal Analysis* vol I (New York: Wiley) p 205
Pope M I and Judd M D 1980 *Differential Thermal Analysis* (London: Heyden) p 49
Rubinstein M and Taylor P C 1974 *Phys. Rev.* B **9** 4258
Thorbjørnsrud J, Ellestad O H, Klæboe P, Torgrimsen T and Christensen D H 1973 *J. Mol. Struct.* **17** 5
Woessner D E and Wutowsky H S 1963 *J. Chem. Phys.* **39** 440
Zuriaga M J and Martín C A 1986 *Z. Naturf.* **41a** 408